Journal of Applied Polymer Science

Thermoplastic Vulcanizate Nanocomposites Based on Thermoplastic Polyurethane and Millable Polyurethane Blends Reinforced with Organoclay Prepared by Melt Intercalation Technique: Optimization of Processing Parameters via Statistical Methods

Aruna Kumar Barick,[1,2] Ji-Yoen Jung,[3] Myung-Chan Choi,[3] Young-Wook Chang[1,3]

[1]Department of Chemical Engineering, Polymer Nano Materials Laboratory, College of Engineering Sciences, Hanyang University, Ansan, Gyeonggi 426-791, Republic of Korea

[2]Research Institute of Engineering and Technology, Research Institute, Research Centers, Hanyang University, Ansan, Gyeonggi 426-791, Republic of Korea

[3]Department of Bio-Nano Technology, College of Engineering Sciences, Hanyang University, Ansan, Gyeonggi 426-791, Republic of Korea

Correspondence to: Y.-W. Chang (E-mail: ywchang@hanyang.ac.kr)

ABSTRACT: Statistical approaches including Taguchi design of experiments (DOE), analysis of variance (ANOVA), and multiple linear regression analysis were employed to determine optimum processing conditions for successful preparation of a thermoplastic vulcanizate nanocomposite (TPVNC) based on thermoplastic polyurethane (TPU)/millable polyurethane (MPU) blend reinforced with an organoclay (TPU/MPU/organoclay = 50/50/3 wt/wt/wt) using an internal mixer. Total numbers of mixing layouts were designed by the application of Taguchi's orthogonal array (OA) methodology based on three parameters and three levels in the L_9 selector matrix model. Mechanical properties of all runs were measured and fitted into the statistical software to determine signal to noise (*S/N*) ratio. Ranks of the parameters were determined based on the delta statistics of the larger is better case of the *S/N* ratio. The ANOVA parameters were analyzed and percentage contribution of each factor, along with the correlation coefficient of each variable, was measured. The multiple linear regression models for each property were correlated with the parameters through mathematical equations. Fourier transform infrared (FTIR) analysis was performed to examine any interfacial interactions between polyurethane matrix and organoclay. X-ray diffraction (XRD) analysis and field emission transmission electron microscope (FETEM) were employed to analyze the dispersion of organoclays in the polymer matrix. Field emission scanning electron microscope (FESEM) was employed to observe cryo-fractured morphology. Dynamic mechanical analysis (DMA) and dynamic shear rheometer (DSR) were used to investigate dynamic mechanical properties and rheological properties of the trials, respectively. Based on all of these characterizations, an optimum processing condition was determined. © 2012 Wiley Periodicals, Inc. J. Appl. Polym. Sci. 129: 1405–1416, 2013

KEYWORDS: clay; mechanical properties; polyurethanes

Received 25 July 2012; accepted 19 November 2012; published online 10 December 2012
DOI: 10.1002/app.38852

INTRODUCTION

Thermoplastic elastomer (TPE) is a special class of polymeric material having both thermoplastic and elastomeric properties such as good elastic characteristics, recyclability, melt processability, and easy moldability. Thermoplastic vulcanizates (TPV) is a blend-based TPE prepared by mixing two different polymers and crosslinking a selective phase in the blend during the mixing, known as a dynamic vulcanization. TPV has excellent elastic properties like rubbers as well as recyclability and melt processibility like thermoplastics.[1]

In the recent decades, TPV/inorganic nanocomposites have been widely studied to enhance material properties of the TPV. TPV based on polypropylene (PP)/ethylene-propylene-diene monomer (EPDM) blend reinforced with several nanofillers such as organoclay,[2–7] silica,[8,9] graphite and its derivatives,[10,11] and bohemite alumina[12] was reported. Effects of type of nanofillers, compatibilizers, and vulcanization systems on material properties of the nanocomposites were investigated in the studies. TPV based on ethylene vinyl acetate (EVA)/natural rubber (NR) blends and PP/epoxidized natural rubber (ENR) blends reinforced with organoclay were also studied.[13,14]

Processing parameters may affect overall properties of end products; hence, these parameters need to be optimized to control the properties and to improve cost and reliability of the products. For successful preparation of the TPV nanocomposites using an internal batch mixer, processing parameters such as mixing temperature, mixing time, and rotor speed are to be optimized. The most trustworthy and practical method to optimize the processing parameters is a statistical approach. Several models have been invented for the statistical approach, which include factorial design,[16] response surface methodology,[17] and Taguchi approach.[18] Among these methods, Taguchi DOE is used commonly due to its easiness and reliability.[19] It employs an orthogonal array to investigate the effects of processing parameters using a small number of experiments. It is the most practical method to investigate the effects of multiple factors on performance properties of samples and to evaluate the influence of individual factors based on the properties. Optimization of processing parameters for melt blending of different polymer blend systems using the Taguchi methodology have been reported in literatures.[18,20–23] Recently, processing parameters for melt mixing of PP/EPDM/organoclay nanocomposites were optimized using the Taguchi analysis method.[24]

The aim of this study is to optimize the processing parameters (mixing temperature, mixing time, and rotor speed) based on the Taguchi method for preparation of organoclay reinforced thermoplastic polyurethane(TPU)/millable polyurethane(MPU) blend TPV using an internal batch mixing method. A particular blend nanocomposite composition (TPU/MPU/organoclay = 50/50/3 wt/wt/wt) was used for the optimization process. The blend nanocomposite samples were prepared using an internal batch mixer with varying processing conditions as per the L_9 OA. The optimum mixing conditions were determined on the basis of tensile properties of each run as response variables. Degree of clay dispersion, fracture surface, dynamic mechanical properties, and rheological properties of the TPV/clay nanocomposite samples were examined.

EXPERIMENTAL

Materials

Polyether based TPU elastomer (Neothane® 6185A) with Shore A hardness of 86 ± 2 and density of 1.12 g/cm^3 was purchased from Dongsung Highchem, Seoul, South Korea. The peroxide curable polyether based millable polyurethane elastomer (Millathane® E40) was procured from TSE Industries, Florida. It has a specific gravity of 1.07 and a Mooney viscosity of 30–60 $ML_{(1+4)}$ @ 100°C. The organically modified montmorillonite (Cloisite® 30B) was supplied by Southern Clay Products, TX. It has a density of 1.98 g/cm^3, Braggs d-spacing (d_{001}) of 1.85 nm, and methyl bis-2-hydroxyethyltallow ammonium (MT2EtOH) organic modifier concentration of 90 meq/100 g with a tallow composition of ~ 65% C18; ~ 30% C16; ~ 5% C14. Dicumyl peroxide (DCP) used as a curing agent have a molecular weight of 270.37, density of 1.56 g/mL at 25°C, and melting point in the range of 39–41°C was purchased from Sigma-Aldrich LLC, Missouri, USA. Triallyl cyanurate (TAC) used as a coagent in peroxide curing have a molecular weight of 249.27, density of 1.11 g/cm^3 at 30°C, and melting point in the range of 26–28°C and was purchased from Tokyo Chemical Industry, Tokyo, Japan.

Table I. Level of Factors Designed for Blending in Internal Batch Mixture

			Level		
Factor code	Control factor	Unit	1	2	3
A	Temperature	°C	180	190	200
B	Rotor Speed	rpm	60	80	100
C	Mixing Time	min	6	8	10

Methods

Taguchi Experimental Design Approach. Taguchi[25] popularized the DOE statistical approach which was originally suggested by Fisher[26] in the 1920s. The Taguchi method is a convenient technique for designing and performing experiments to investigate and evaluate processing parameters. The primary focus of the Taguchi robust DOE is to improve the process, yield, performance, and quality of the products by optimizing the effects of control and noise factors on the product design. It is one of the most promising scientific routes available to improve product quality, reduce product cost, and reduce the time interval between design and successful industrial implementation.[27]

Selection of the Processing Parameters and Their Levels. The dynamically vulcanized TPU/MPU blend nanocomposite samples were prepared using an internal batch mixer. General processing parameters associated with batch mixing are mixing temperature, mixing time, and rotor speed. In the present work, three factors at three levels were considered as shown in Table I. The ranges for the levels of factors were selected in light of data available in the literatures, material data sheets, and polymer handbooks.

Selection of Orthogonal Array. The processing parameters consist of three factors and three levels have $3^3 = 27$ possible combinations of trials for a full factorial design. It is difficult to conduct all 27 experiments. The Taguchi DOE method is based on highly fractional orthogonal designs, which follow "orthogonal array testing strategy (OATS)" or "orthogonal array selector matrix (OASM)" techniques to propose an appropriate OA to allocate a laboratory or industrial experiment with many variable parameters and a small number of trials.[28] Selection of a typical OA for different independent variables involves each variable having different values depending on the total degrees of freedom (DOF) of the parameters. The DOF of the parameter is an important factor for statistical analysis, as it determines optimal level.[19] Each factor has three individual levels, so the total number of DOF for the parameters is six. Generally the DOF value for the OA must be greater than or equal to number of processing parameters. Here, the selected OA is L_9 (3^3), as shown in Table II, with eight experimental DOF, which is higher than the DOF of the parameters. Tensile properties (strength, modulus, and elongation-at-break) are considered as main response characteristics for evaluation of the quality of the mixing process.

Table II. L_9 Orthogonal Array of Taguchi Method

Experiment number	A	B	C
1	1	1	1
2	1	2	2
3	1	3	3
4	2	1	2
5	2	2	3
6	2	3	1
7	3	1	3
8	3	2	1
9	3	3	2

Processing

Preparation of TPU/MPU/Organoclay-Based TPVNC. TPU/MPU/organoclay (50/50/3 wt/wt/wt) blend nanocomposite samples were prepared by melt blending the polymers and a clay using a Haake internal mixer (Rheomix 600P, Haake, NJ) equipped with a cam rotor. DCP (6 phr) and TAC (2 phr) were added during the mixing to induce vulcanization in MPU phase. The compounding was carried out with fill factor of 0.7 at different combination of mixing temperature, mixing time, and rotor speed. The experiment was designed on the basis of L_9 OA as shown in Table III. Polymers and an organoclay were dried before processing in a preheated vacuum oven for 24 h before compounding. The prepared TPVNC samples were compression molded to form a sheet about 1–2 mm thickness using a laboratory scale heating press (Type MH 15, Masada Seisakusho, Tokyo, Japan) at 180°C for 10 min at a pressure of 15 MPa. The compression molded sheets were cooled to room temperature under adequate pressure and were then kept in a vacuum oven for 72 h at 50°C for post curing. Samples for tensile testing, DMA, and rheological analysis were punched out from the sheet.

Measurement and Characterizations. Tensile properties of the TPVNC specimens were determined at room temperature according to the ASTM D-412-98 test procedure using dumbbell-shaped specimens with a universal testing machine (UTM) (STM-10E, United Calibration Corporation, CA) at a crosshead speed of 50 mm/min. Five samples were tested for each trial, and the average of the data was reported. FTIR spectrometer (Nicolet 6700, Thermo Fisher Scientific, MA) equipped with an attenuated total reflectance (ATR) accessory was used to evaluate the interfacial interactions between organoclay and polyurethane matrices. FTIR spectra were recorded in dispersive mode over a range of 400–4000 cm^{-1} at a resolution of 4 cm^{-1}. Sixteen scans were collected per trace. XRD patterns of the TPVNC samples were obtained using X-ray diffractometer (D/MAX-2500/PC, Rigaku Corporation, Tokyo, Japan) operated at a voltage of 40 kV and current of 30 mA with a Cu-$K_{\alpha 1}$ (λ = 0.1540598 nm) radiation source. The experiment was performed over a scan range of 2θ = 2.0–10° at a scan rate of 2°/min and step size of 0.02° at room temperature. Morphology of the cryo-fractured surface of the TPVNC samples was examined by FESEM (MIRA3 LM, Tescan USA, PA) at an accelerating voltage of 30 kV and probe current of 100 nA. The sample surfaces were platinum coated by means of a manually operated sputter coater. Morphology of the TPVNC was examined by FETEM (JEM-2100F, JEOL, Tokyo, Japan) at an acceleration voltage of 200 kV. The cryo ultramicrotome (PT-PC PowerTome Ultramicrotomes, Boeckeler Instruments, AZ) was employed for preparation of ultra-thin sections less than 100 nm. Dynamic mechanical properties of the TPVNC were measured by DMA (DMA Q800, TA Instruments, DE) in the temperature range of −100 to +250°C at an applied frequency of 1 Hz and strain amplitude of 10 μm with a scan rate of 2°C/min. Rheological behaviors of the TPVNC samples were investigated by DSR (advanced rheometric expansion system (ARES), Rheometrics, NJ) using a set of 25 mm diameter parallel plates with a sample of 1–2 mm thickness and 25 mm diameter. The frequency sweep was carried out within the frequency range of 10^{-1}–10^{2} rad/s at 180°C with a strain of 0.5%, which is well within the linear viscoelastic region.

DATA ANALYSIS, RESULTS, AND DISCUSSION

Tensile Properties

The modulus at 150% elongation, elongation at break, and tensile strength of different trials for the TPVNC are shown in Table IV. Quantitative values specified to 4–5 digits after the decimal point to correctly differentiate entries from each other. In Table IV, it can be seen that the highest tensile strength and modulus at 150% elongation was obtained in Run1. This indicates that adequate mixing of TPU and MPU and good dispersion of the organoclays were achieved at the processing condition. On the other hand, elongation-at-break shows the highest value in Run6, which may be associated with nanofiller orientation along a particular direction.

Analysis of the Taguchi Methodology of TPVNC

Signal to Noise Ratio (S/N). Taguchi design method utilizes quality loss function to determine quality characteristics.[29] It is a continuous mathematical function that is defined in terms of the deviation of a design parameter from an ideal or target value. Taguchi's loss function is expressed in the form of a quadratic relationship in the following equation:

$$L(y) = k(\mathrm{MSD}) = k(y - m)^2 \quad (1)$$

Table III. Experimental Layout Based on Taguchi L_9 Orthogonal Array Model

Experiment number	Temperature (°C)	Rotor speed (rpm)	Mixing time (min)
Run1	180	60	6
Run2	180	80	8
Run3	180	100	10
Run4	190	60	8
Run5	190	80	10
Run6	190	100	6
Run7	200	60	10
Run8	200	80	6
Run9	200	100	8

Table IV. Tensile Properties of TPU/MPU/C30B Vulcanizate Nanocomposites

Experiment number	Tensile Strength (MPa)	Elongation at break (%)	Modulus at 150% elongation (MPa)
Run1	6.24335 ± 0.1045	275.5016 ± 07.0494	3.60056 ± 0.0900
Run2	5.92034 ± 0.3576	298.3806 ± 19.2681	3.07580 ± 0.2263
Run3	4.83550 ± 0.1890	340.7100 ± 20.6781	2.57580 ± 0.0735
Run4	5.31227 ± 0.2787	339.3373 ± 35.1130	2.68665 ± 0.1307
Run5	4.42222 ± 0.1285	338.3847 ± 15.4485	2.43952 ± 0.0497
Run6	5.35908 ± 0.1304	370.7660 ± 25.0472	2.58952 ± 0.0634
Run7	4.27202 ± 0.2002	351.5660 ± 22.8172	2.23452 ± 0.0391
Run8	4.75030 ± 0.2506	369.3251 ± 34.3498	2.43192 ± 0.0221
Run9	4.27144 ± 0.2289	358.734 ± 21.1313	2.28380 ± 0.0412

where, "y" is critical performance parameter value, "L" is loss associated with a particular parameter "y" and "m" is nominal or target value of the specified parameter, "MSD" is mean squared deviation, and "k" is a constant that depends on the cost at the specification limits, which is determined conventionally by dividing the cost of the product by the square of the lower or higher tolerance values.

The quality loss function values may be expressed by generic "signal to noise" (S/N) ratio (η). There are three types of noise factors, which are outer noise, inner noise, and between the product noises. The "signal" represents desirable value (mean) for the output, and the "noise" represents undesirable value [signal disturbance and standard deviation (SD)] for the output.[30] Taguchi method promoted the concept of the "inner array" and "outer array", which consist of the OA that contains the control and noise factors settings, respectively, for successive implementation of the design approach. Combination of both arrays constitutes the "product array" or "complete parameter design layout".[31] The mean response and standard deviation for each trial are estimated by using the following equations.

$$\text{Mean response}(\bar{y}) = \frac{1}{n}\left(\sum_{i=1}^{n} y_i\right) \tag{2}$$

Table V. S/N Ratios of Individual Trials

	Response performance		
Experimental number	Tensile strength (MPa)	Modulus at 150% elongation (MPa)	Elongation at break (%)
Run1	15.9084	11.1274	48.8025
Run2	15.4469	9.7592	49.4954
Run3	13.6888	8.2182	50.6477
Run4	14.5056	8.5842	50.6126
Run5	12.9128	7.7461	50.5882
Run6	14.5818	8.2644	51.3820
Run7	12.6127	6.9837	50.9201
Run8	13.5344	7.7190	51.3482
Run9	12.6115	7.1732	51.0955

$$\text{Standard deviation(SD)} = \sqrt{\sum_{i=1}^{n} \frac{(y_i - \bar{y})^2}{n-1}} \tag{3}$$

The noise factors are mainly responsible for causing a product's end use performance to deviate from its target value. Therefore, primary aim of Taguchi parameter design approach deals with a selection of appropriate control factors, which makes the product more reliable since it is unaffected by deviation due to noise factors. Taguchi robust design method adopts the S/N ratio to investigate the deviation of quality characteristic values from the degree of expected performance of a product or process. The highest S/N ratio for the product design always determines the optimum quality of characteristic signals with the least variation around the target parameter due to the random effects of the noise factors. The quality loss function generally implements three standard quality characteristics known as "nominal the best," "smaller the better," and "larger the better" to estimate the S/N ratio.[30] These characteristics are defined by different sets of equations that distinguish them from general loss function equation. Numerically, the "smaller the better" makes the system response as small as possible as stated in the equation below:

$$\eta = S/N_S = -10\log\frac{1}{n}\left(\sum_{i=1}^{n} y_i^2\right) \tag{4}$$

where, "n" is the number of experiments and "y_i" is the measured property for the ith experiment.

Mathematical expression for "nominal the best" to reduce variability around a target is represented in following equation:

$$\eta = S/N_T = 10\log\left(\frac{\bar{y}^2}{S^2}\right) \tag{5}$$

The "larger the better" concept to make the system response as large as possible is adopted to determine S/N ratio values in this article. It is represented in following equation:

$$\eta = S/N_L = -10\log\frac{1}{n}\left(\sum_{i=1}^{n} \frac{1}{y_i^2}\right) \tag{6}$$

The loss function equation used for the "larger the better" to depict the loss function of one unit of product is stated below:

Table VI. Values of S/N Ratios of Tensile Properties of TPU/MPU/C30B Vulcanizate Nanocomposites

Test	Level	Temperature	Rotor speed	Mixing time
Tensile strength	Level1	15.01	14.34	14.67
	Level2	14.00	13.96	14.19
	Level3	12.92	13.63	13.07
	Delta	2.10	0.71	1.60
	Rank	1	3	2
Elongation at break	Level1	49.65	50.11	50.51
	Level2	50.86	50.48	50.40
	Level3	51.12	51.04	50.72
	Delta	1.47	0.93	0.32
	Rank	1	2	3
Modulus at 150% elongation	Level1	9.702	8.898	9.037
	Level2	8.198	8.408	8.506
	Level3	7.292	7.885	7.649
	Delta	2.410	1.013	1.388
	Rank	1	3	2

$$L = k/y_0^2 \tag{7}$$

where, "k" is the proportionality constant and "y_0" is the minimum product tolerated output value. The S/N ratio corresponds to the each design points for all the 9 trial conditions are calculated based on the Equation 6 as shown in Table V.

The *S/N* ratio corresponds to the design points for all nine trial conditions as calculated according to the above equation. Table VI represents the values of mean *S/N* ratios at low and high levels of tensile properties of TPVNC. The *S/N* ratios of each level of the respective parameters are tabulated for the system. Rank of parameters is determined by the delta (Δ) value, which is calculated as given below:

$$\Delta = (\max(S/N)) - (\min(S/N)) \tag{8}$$

The control factor with the strongest influence on response was determined by the difference values of *S/N* ratios (Δ). The larger the difference, the more the control factor impacts the response, or the stronger interactions exist between the two controlling factors. The main effect plots for the *S/N* ratios are shown in Figure 1(a–c). The main effect plots clearly indicate that the design parameters significantly influence the mean of the *S/N* ratios. The highest *S/N* ratios of processing parameters for tensile strength (σ_b) and modulus at 150% elongation (M_{150}) responses are matched with Run1, which consist of mixing temperature of 180°C, mixing time of 6 min, and rotor speed of 60 rpm, which resemble Run1 of the OA. It is not necessary to carry out a confirmation test. The values of both σ_b and M_{150} decreased with the increase in processing parameters, which may be due to the polymer chain scission and degradation at the processing conditions. Values of *S/N* ratios significantly decreased as the magnitude of the processing parameters

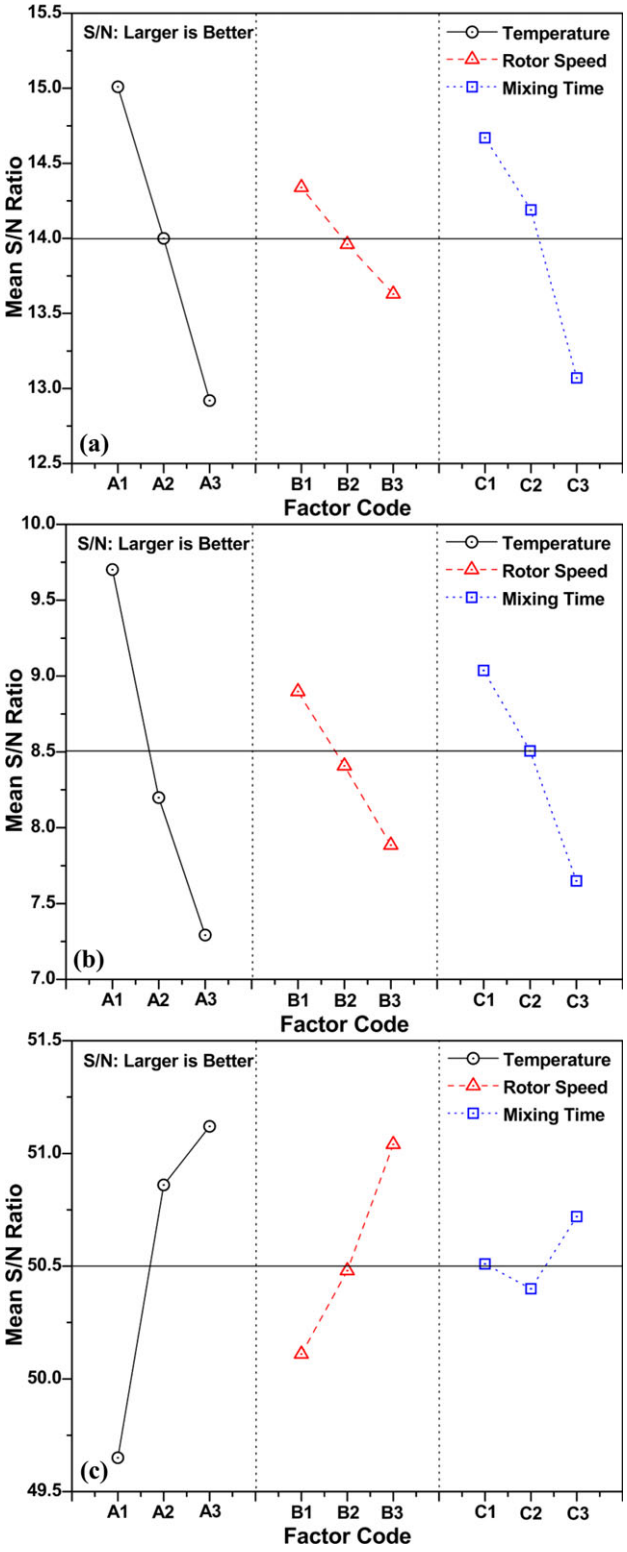

Figure 1. Main effects plot for *S/N* ratios of (a) tensile strength (b) modulus at 150% elongation, and (c) elongation at break. [Color figure can be viewed in the online issue, which is available at wileyonlinelibrary.com.]

increased, which indicates that the higher magnitude processing conditions deteriorate the performance properties. The delta value determines the rank of the factors such that the highest delta value can be attributed to the highest rank. The S/N ratio analysis assigns the highest rank to the mixing temperature, which confirmed that major processing factor is temperature. The next important factor is mixing time, and the least important factor is rotor speed. However, the highest S/N ratios of processing parameters for elongation at break (ε_b) are the same at Run3, which has a mixing temperature of 200°C, mixing time of 10 min, and rotor speed of 100 rpm, which is not matched with OA. A confirmation test was carried out to determine percentage error between predicted data and experimental data. From the *S/N* analysis, it is concluded that mixing temperature is the most important factor to affect the material properties, and mixing time and rotor speed get second and third priorities, respectively.

Analysis of Variance (ANOVA) Study

Analysis of variance (ANOVA) is a routinely used standard statistical objective decision making technique to identify the presence of any differences in the average performance characteristics of group of items measured simultaneously.[32] The ANOVA proposes three statistical factors (i) relative influence of both factors and interactions, (ii) confidence interval level estimation based on performance at optimum conditions and main effects, and (iii) significance of influence of factor and interaction. Main purpose of ANOVA is to detect differences among variables, assuming that the control factors significantly influence the responsive performances. The ANOVA tool is performed by the partition of the total variability (variance) in the quality performance into identifiable sources of variations and the associated degrees of freedom in an experiment. It is measured by the sum of the squared deviations from the total mean of the quality characteristics, along with contributions from each of the factors under investigation (control factors) and total experimental errors (noise factors) at specific confidence intervals. The robust design conditions can be well predicted by understanding the source and magnitude of the variance. The total sum of squared deviations (SS_T) is the sum of squares of the difference of the dependent variables of the mean. The SS_T is divided into two variances, which can be explained in terms of a regression equation (sum of squared deviation (SS_D) due to individual design parameter) or attributed to random errors [sum of squares of error (SS_E)].[33] The SS_T from the total mean S/N ratio (η_m) can be calculated by following equation:

$$SS_T = SS_D + SS_E \tag{9}$$

$$SS_T = \sum_{i=1}^{n} (y_i - \overline{y})^2 = \sum_{i=1}^{n} (y_i - \overline{y})^2 + \sum_{i=1}^{n} e_i^2 \tag{10}$$

where, $\overline{y}$ is the average of y_i.

The percentage contribution of each factor (ρ_i) on the performance properties is calculated by following equation:

$$\rho_i(\%) = (SS_K/SS_T) \times 100 \tag{11}$$

where, SS_K is the sum of squares of parameter "*K*".

In this study, ANOVA is used to analyze the effects of processing parameters such as mixing temperature, mixing time, and rotor speed on tensile properties of the TPVNC. Results of ANOVA for the tensile properties are presented in Table VII. Relative importance of the processing parameters with respect to tensile properties was extensively investigated to determine optimum combination of processing parameters, more accurately by applying ANOVA. The ANOVA *F*-test provides a decisive state for a fixed confidence level. The magnitudes of the "*F*" parameter significantly differentiate the importance of the individual processing parameters. It is noted in Table VII that the "*F*" values for the mixing temperature for each case had the highest score, which shows that mixing temperature has the largest effect on the performance. Statistical parameter "*P*" also ranks the processing parameters, in which the lowest value contributes most significantly to performance properties. The percentage contribution indicates a relative power of a control factor to reduce variation. A processing factor with the highest percentage of contribution has the greatest influence on performance even at a level of variation. As can be seen in Table VII, mixing temperature greatly affects the response properties, while mixing time and rotor speed have minimal effect on the performance. It is worth mentioning that the values of percentage contribution of the design parameters are consistent with the assigned rank of parameters calculated from *S/N* ratios. Values of the coefficient of determination (R^2) are satisfactory, which confirms that data fit well into the ANOVA analysis (fitting between the general linear model and experimental data), and the obtained results have practical relevance.

Interaction of Design Parameters

True estimation of interactions of control factors (factors in the inner array) is achieved when noise factors (factors in the outer array) are considered together. Interpretation of the main effects on the processing conditions becomes incomplete and misleading in the presence of interactions. The interactions arise when the combined effects of several factors on the measurement of the design parameters are larger or smaller than the sum of their individual effects. On the other hand, the influence of a chosen factor is in association with other factors.[34] The ANOVA has the capability to evaluate and test the effects of interactions. Parallel interaction plots indicates the absence of interaction among parameters, whereas nonparallel lines, which may cross each other, indicate a presence of significant interactions between them.[35] The interaction plots for tensile properties of the processing parameters of TPVNC are shown in Figure 2(a–c). The lines are not straight and also are not parallel to each other, which indicate the presence of significant interactions between the processing parameters. The interaction effect is significant with the ordinal interaction (slope of lines not parallel and do not cross), so the main effect of control factors may be interpreted and tested acceptably. However, the main effects cannot be estimated correctly in the case of disordinal interaction (lines cross each other). Processing parameters such as mixing temperature, mixing time, and rotor speed have strong interactions, as shown in the figures. Hence, appropriate selection of the optimized processing parameters may minimize the interactions among them. The main effect of these factors is the

Table VII. Analysis of Variance of Processing Parameters of TPU/MPU/C30B Vulcanizate Nanocomposites

Test	Factors	DF	Seq SS	Adj SS	Adj MS	F	P	ρ_i
Tensile Strength	Temperature	2	2.28899	2.28899	1.14450	25.56	0.038	56.00948
	Rotor speed	2	0.30965	0.30965	0.15482	3.46	0.224	7.576851
	Mixing time	2	1.39860	1.39860	0.69930	15.62	0.060	34.22245
	Error	2	0.08955	0.08955	0.04477			2.191206
	Total	8	4.08679					100.00
		$S = 0.211599$; $R^2 = 97.81\%$; $R^2(\text{adj}) = 91.24\%$						
Elongation at break	Temperature	2	5125.9	5125.9	2563.0	5.11	0.164	62.86516
	Rotor speed	2	1829.1	1829.1	914.5	1.82	0.354	22.43248
	Mixing time	2	196.0	196.0	98.0	0.20	0.837	2.403787
	Error	2	1002.8	1002.8	501.4			12.29856
	Total	8	8153.8					100.00
		$S = 22.3919$; $R^2 = 87.70\%$; $R^2(\text{adj}) = 50.81\%$						
Modulus at 150% elongation	Temperature	2	0.91616	0.91616	0.45808	13.34	0.070	61.34520
	Rotor speed	2	0.19207	0.19207	0.09604	2.80	0.263	12.86082
	Mixing time	2	0.31651	0.31651	0.15826	4.61	0.178	21.19321
	Error	2	0.06870	0.06870	0.03435			4.600087
	Total	8	1.49345					100.00
		$S = 0.185338$; $R^2 = 95.40\%$; $R^2(\text{adj}) = 81.60\%$						

Adj MS, adjusted means squares; Adj SS, adjusted (partial) sums of squares; DF, degrees of freedom; Seq SS, sequential sums of squares.

mutual final effect imparted by the individual processing parameters.

Multiple Linear Regression Analysis

Multiple linear regression (MLR) is a statistical technique widely used to predict a theoretical model and establishes a linear relationship between the dependent variables (predicted values) and one or more independent variables (predictors). This model is based on the least square method to fit the data into a straight line, where the sum of squares of vertical deviation for observed and predicted values may be minimized.[36] The general mathematical expression for the MLR model is illustrated below:

$$y = b_0 + \sum_{i=1}^{n} b_i x_i \quad (12)$$

where, y is dependent variable, b_0 is intercept or constant term, x_i is ith independent variable from total set of "n" number of independent variables (number of coefficients), and b_i is ith coefficient corresponding to x_i.

The MLR analysis was employed to determine a linear equation for the tensile strength of TPVNC as a function of processing parameters. In this case, dependent variables are tensile properties and independent variables are processing parameters. Mathematical models for tensile properties were derived by considering these factors, and their interactions are shown in the equations below:

$$\text{TS} = 19.6 - 0.0618\ \text{Temperature} - 0.0113\ \text{Rotor Speed} - 0.235\ \text{Mixing Time} \quad (13)$$

$$\text{EB} = -264 + 2.75\ \text{Temperature} + 0.865\ \text{Rotor Speed} + 1.26\ \text{Mixing Time} \quad (14)$$

$$M_{150} = 11.6 - 0.0384\ \text{Temperature} - 0.00894\ \text{Rotor Speed} - 0.114\ \text{Mixing Time} \quad (15)$$

These equations suggest that the tensile properties are the sum of contributions of individual parameters. The coefficients of determination (R^2) of the fitting lines are 96.1%, 78.2%, and 93.0%, respectively. This MLR analysis quantitatively estimates the contribution or synergistic effect of each individual processing parameter on the responses.

Confirmation Test

Experimental confirmation test is a final step for verification of responsive properties derived from Taguchi method. The larger the better signals of *S/N* ratio are considered for the optimized processing parameter due to their highest contribution to the tensile properties. The optimized conditions for obtaining highest tensile strength and modulus are mixing temperature of 180°C, mixing time of 6 min, and rotor speed of 60 rpm, which is one of the exact processing combinations present in L_9 OA. The optimized conditions for obtaining highest elongation-at-break are mixing temperature of 200°C, mixing time of 10 min, and rotor speed of 100 rpm, which allows error between the theoretical prediction and practical evaluation. Table VIII shows values of confirmation tests and their comparison with the MLR model for quality controls.

Applied Polymer SCIENCE

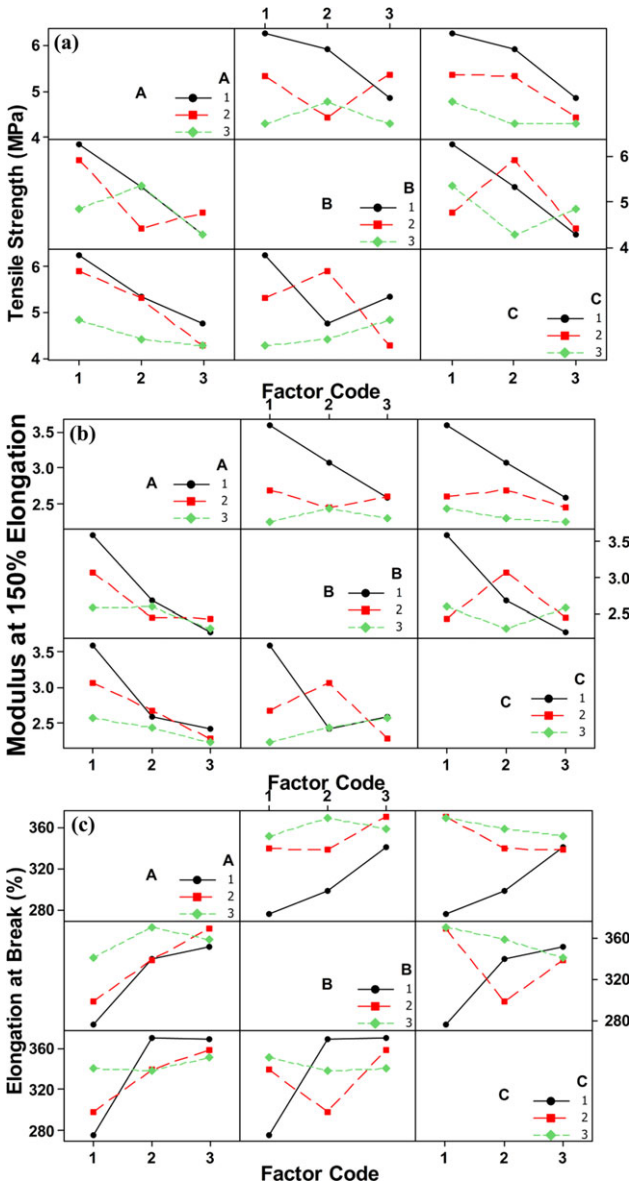

Figure 2. Interaction plots for (a) tensile strength (b) modulus at 150% elongation, and (c) elongation at break. [Color figure can be viewed in the online issue, which is available at wileyonlinelibrary.com.]

Microstructure Analysis

FTIR spectra of the different trials are shown in Figure 3(a,b). Figure 3(a) shows the absorption bands at 1703 cm^{-1} and 1729 cm^{-1}, which are assigned to stretching vibration of hydrogen bonded and free >C═O of urethane bond, respectively. The result indicates that the >C═O of urethane linkage is hydrogen bonded with hydroxyl groups (—OH) present on the organoclays.[37,38] Figure 3(b) shows a strong broad band centered at around 3308 cm^{-1} and a small shoulder at about 3450 cm^{-1}, which are attributed to the hydrogen bonded and free N—H symmetric stretching of urethane bond, which indicates that N—H group in urethane bond is hydrogen-bonded with the >C═O and —C—O—C— of polyurethane and oxygen of the hydroxyl groups (—OH) present on organoclays.[39]

Table VIII. Confirmation Tests and Their Comparison with Regression Model

Test	Predicted	Experimental	% Error
Tensile strength	6.388	6.24335	2.26440
Elongation at break	385.1	370.3457	3.98392
Modulus at 150% elongation	3.4676	3.60056	3.83435

XRD patterns of all the trials and pristine Cloisite 30B are shown in Figure 4. The XRD pattern of Cloisite 30B showed a prominent peak at $2\theta = 4.78°$ and a small broad peak at $2\theta = 9.56°$, which correspond to $d_{001} = 1.8472$ nm and $d_{002} = 0.9244$ nm Bragg reflection planes, respectively.[40] The diffraction peaks are completely disappeared in the XRD pattern of 3 wt % Cloisite 30B-filled TPU/MPU blend system for all the trials irrespective of the processing conditions, which indicates that the clay layers are completely exfoliated in the polymer matrices. The driving force to induce extensive intercalation of the polymer into the layers of

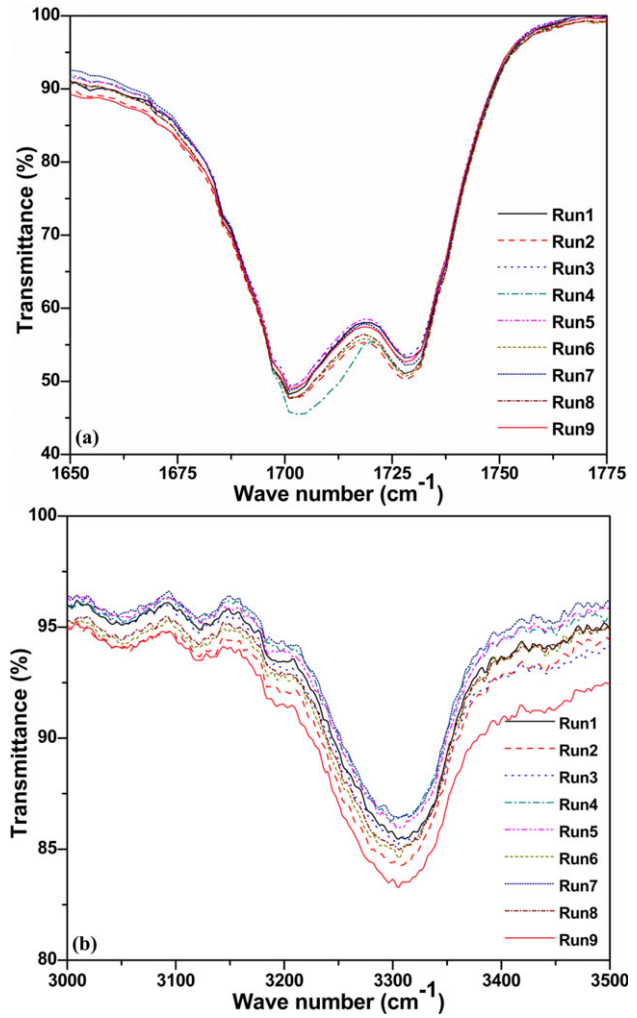

Figure 3. FTIR spectra of (a) carbonyl and (b) amine stretching regions of urethane linkage of polyurethane matrices for all trials. [Color figure can be viewed in the online issue, which is available at wileyonlinelibrary.com.]

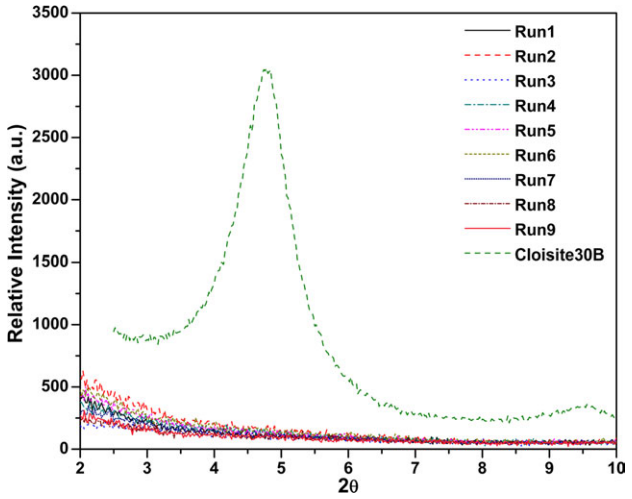

Figure 4. XRD graphs of all trials. [Color figure can be viewed in the online issue, which is available at wileyonlinelibrary.com.]

organoclays is hydrogen bonding interaction between the organoclay and polyurethanes. When the sufficient compatibility is met, thermoplastics/organoclay nanocomposites with the exfoliated structure can be formed by a high shear mixing.[41,42] Paul and Robeson[41] have represented the mechanism of dispersion of organoclays in a polymer matrix during high shear melt mixing.[41] Our studies showed that processing conditions optimized by Taguchi methodology are suitable to produce uniform dispersion of the organoclays in polyurethane matrices.

Cryo-Fractured Morphology

Cryo-fractured surfaces of samples are shown in Figure 5. It can be seen that surface roughness of the fractured samples varied with processing parameters. Samples prepared at low temperature exhibit high surface roughness while the samples fabricated at high temperature show relatively smooth fracture surface, and this trend is relevant to tensile properties. Any filler aggregates were not observed in the fracture morphology indicating a well dispersion of the organoclays in matrix polymer.

Nanostructured Morphology

TEM micrographs of all trials are shown in Figure 6. It is observed that the organoclays are homogeneously dispersed at nanometer scale in polyurethane matrices. These observations indicate that processing conditions determined from the Taguchi DOE methodology, which are mixing temperature of 180°C,

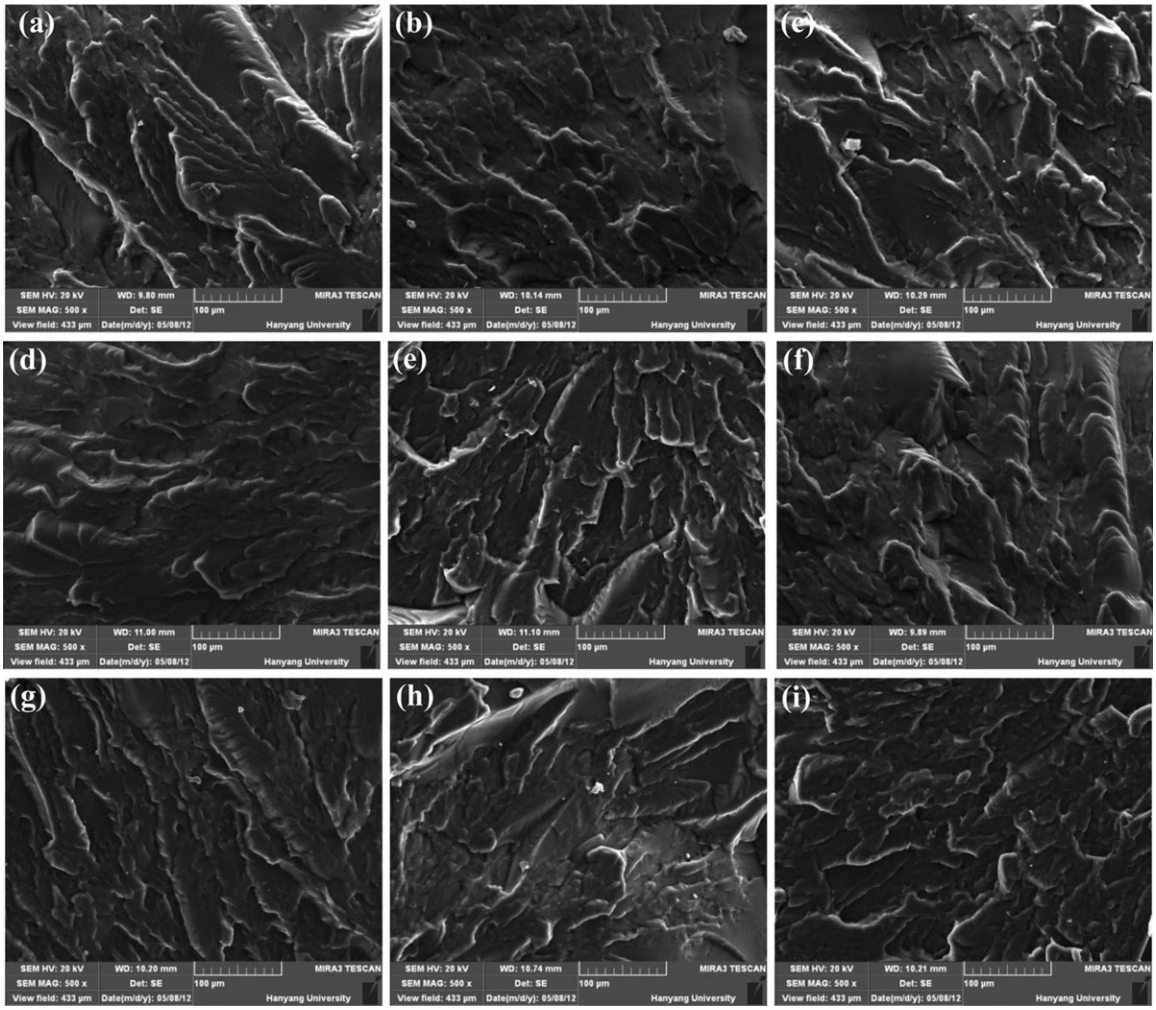

Figure 5. FESEM microphotographs of (a) Run1, (b) Run2, (c) Run3, (d) Run4, (e) Run5, (f) Run6, (g) Run7, (h) Run8, and (i) Run9.

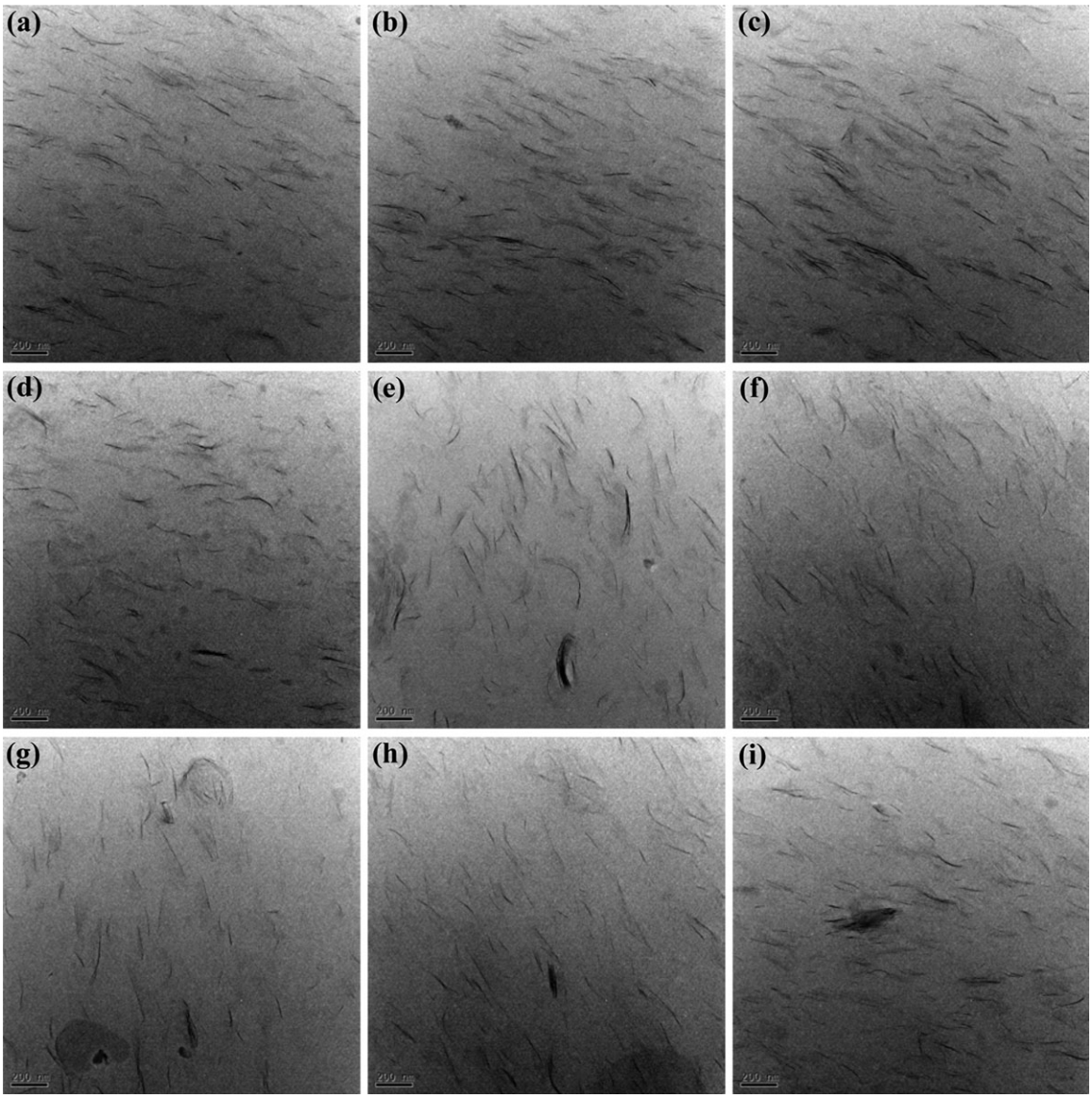

Figure 6. FETEM microphotographs of (a) Run1, (b) Run2, (c) Run3, (d) Run4, (e) Run5, (f) Run6, (g) Run7, (h) Run8, and (i) Run9.

mixing time of 6 min, and rotor speed of 60 rpm, are well adapted to achieve nanoscaled dispersion of the clays in matrix polymer.

Dynamic Mechanical Properties

Figure 7(a,b) represents variation of dynamic storage modulus (E') and damping behavior (tan δ) of samples with temperature. Figure 7(a) shows that E' value rapidly drops around -50°C, which corresponds to T_g of the matrix polymer and E' value gradually decreases with increasing temperature. Run1 samples show that E' value of samples are affected noticeably by processing parameters (mixing temperature, mixing time, and rotor speed). The modulus of all the trials decreases with increasing processing parameters, which is more prominent at elevated temperature region. Hence, preparation of TPVNC should be carried out at a suitable condition to achieve high reinforcing effect.

Figure 7(b) shows that tan δ value is the lowest in Run1, and it increases with increasing processing parameters. The figure also shows that the tan δ peak shifts to lower temperature region with increase in mixing temperature, mixing time, and mixing speed. These results show that optimized processing condition drawn by statistical method is in good agreement with the variation of DMA results.

Rheological Properties

Variation of shear storage modulus (G') and complex viscosity (η^*) of samples in melt state with applied angular frequency are shown in Figure 8(a,b). It is observed in Figure 8(a) that the value of G' increases with increasing frequency within the measured frequency range, which is correlated with a change in relaxation time with frequency. At low frequency region, the relaxation time is large and polymer chains have sufficient time to be relaxed, while at high frequency region the polymer chains don't have enough time to be relaxed under an imposed

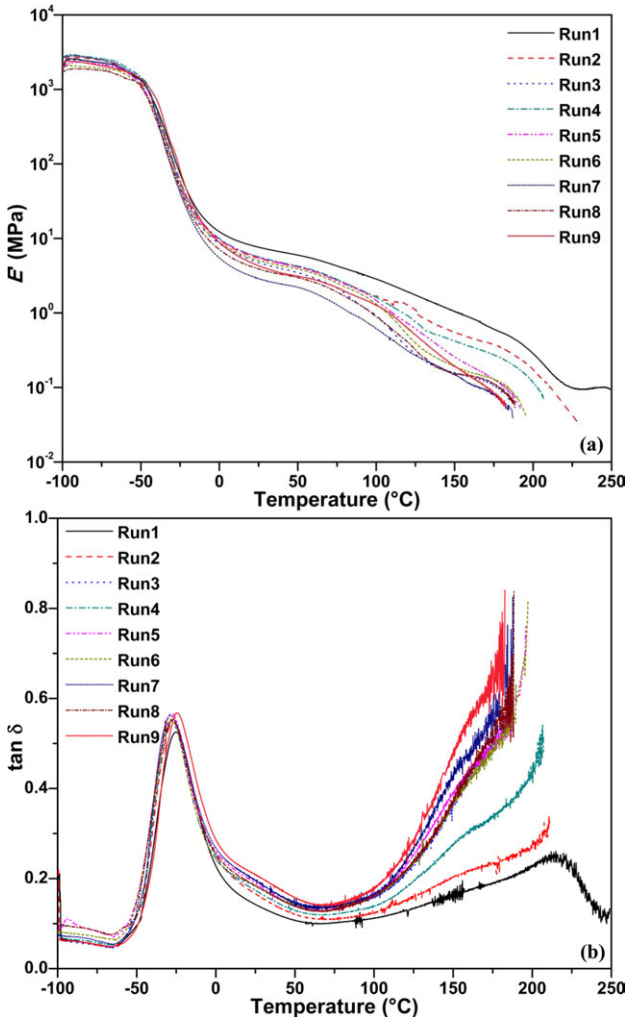

Figure 7. DMA thermograms of (a) E' and (b) tan δ of all trails. [Color figure can be viewed in the online issue, which is available at wileyonlinelibrary.com.]

dynamic stress.[43] The value of G' is the highest for Run1, and it decreases with increase in mixing temperature, time of mixing, and rotor speed, which may be due to breakdown and degradation of polymer chains at higher values of processing parameters.

Figure 8(b) shows that η^* gradually decreases with increase in applied frequency. This is well known as shear thinning behavior and is typically observed in molten thermoplastics.[44,45] At low frequency region, nanofillers tend to resist the flow of polymer melt due to their strong interfacial interactions with matrix polymer chains, while at higher frequency region the resistance to flow is reduced because the clay nanoparticles are aligned along the direction of the flow.[11] The figure also shows that the highest η^* value was obtained in Run1 and the η^* value reduces with increase in mixing temperature, mixing time, and rotor speed, which may be due to breakdown and degradation of polymer chains at higher values of processing parameters. The rheological analysis, in combination with mechanical analysis showed that Run1 processing condition is suitable to produce nanocomposite with the desirable performance properties, which is consistent with the results obtained by statistical analysis.

CONCLUSIONS

Optimum processing conditions such as mixing temperature, mixing time and rotor speed were determined based on the L_9 OA using dynamically vulcanized thermoplastic polyurethane/millable polyurethane blend nanocomposites with an organoclay as a sample material. Mechanical properties (tensile strength, elongation at break, modulus at 150% elongation) of the blend nanocomposites were taken as response to determine S/N ratios and optimum processing conditions. Optimized processing conditions established by the DOE methodology were well consistent with microstructure and material properties of the samples. X-ray diffraction (XRD) and transmission electron microscope (TEM) revealed that the samples form nanocomposites in which the organoclays are uniformly dispersed at nanoscale within polymer matrix. It can also be seen

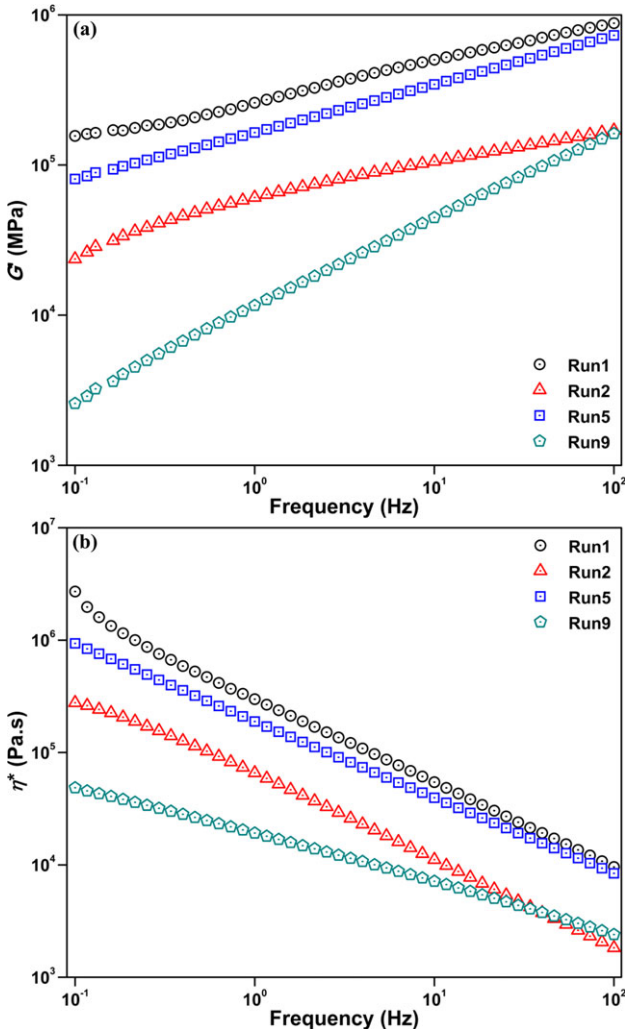

Figure 8. DSR rheographs of (a) G' and (b) η^* of trails. [Color figure can be viewed in the online issue, which is available at wileyonlinelibrary.com.]

that fracture surfaces, dynamic mechanical properties, and rheological properties of the samples are well correlated with the processing parameters.

ACKNOWLEDGMENTS

This work is supported by the research fund of Hanyang University, ERICA Campus, Republic of Korea (HY-2012-P). The post-doctoral research fellowship provided by Hanyang University is gratefully acknowledged by one of the author (A. K. Barick). The authors are heartily thankful to S. Mohapatra and J. A. Gopi of Indian Institute of Technology Kharagpur, India for their help to acquire preliminary knowledge about statistical software analysis.

REFERENCES

1. Tian, M.; Han, J.; Zou, H.; Tian, H.; Wu, H.; She, Q.; Chen, W.; Zhang, L. *J. Polym. Res.* **2012**, *19*, 9745.
2. Lee, K. Y.; Goettler, L. A. *Polym. Eng. Sci.* **2004**, *44*, 1103.
3. Mishra, J. K.; Kim, G.-H.; Kim, I.; Chung, I.-J.; Ha, C.-S. *J. Polym. Sci. Part B: Polym. Phys.* **2004**, *42*, 2900.
4. Mishra, J. K.; Kim, I.; Ha, C.-S. Ryou, J.-H.; Kim, G.-H. *Rubber Chem. Technol.* **2005**, *78*, 42.
5. Mishra, J. K.; Hwang, K.-J.; Ha, C.-S. *Polymer* **2005**, *46*, 1995.
6. Mirzazadeh, H.; Katbab, A. A. *Polym. Adv. Technol.* **2006**, *17*, 975.
7. Saikrasun, S.; Amornsakchai, T. *J. Polym. Res.* **2012**, *19*, 9750.
8. Wu, T.-M.; Chu, M.-S. *J. Appl. Polym. Sci.* **2005**, *98*, 2058.
9. Chatterjee, K.; Naskar, K. *Polym. Eng. Sci.* **2008**, *48*, 1077.
10. Katbab, A. A.; Hrymak, A. N.; Kasmadjian, K. *J. Appl. Polym. Sci.* **2008**, *107*, 3425.
11. Ranjbar, B.; Mirzazadeh, H.; Katbab, A. A.; Hrymak, A. N. *J. Appl. Polym. Sci.* **2012**, *123*, 32.
12. Siengchin, S.; Karger-Kocsis, J. *Compos.: Part A* **2010**, *41*, 768.
13. Munusamy, Y.; Ismail, H.; Mariatti M.; Ratnam, C. T. *J. Reinf. Plast. Compos.* **2008**, *27*, 1925.
14. Ismail, H.; Munusamy, Y.; Jaafar, M.; Ratnam, C. T. *Polym.-Plast. Technol. Eng.* **2008**, *47*, 752.
15. Balakrishnan, H.; Attaran, S. A.; Imran, M.; Hassan, A. Wahit, M. U. *J. Thermoplast. Compos. Mater.* **2012**. DOI: 10.1177/0892705712443252.
16. Tillekeratne, M.; Jollands, M.; Cser, F.; Bhattacharya, S. N. *J. Appl. Polym. Sci.* **2006**, *100*, 2652.
17. Mohamad, N.; Muchtar, A.; Ghazali, M. J.; Mohd, D. H. Azhari, C. H. *J. Appl. Polym. Sci.* **2010**, *115*, 183.
18. Gopi, J. A.; Nando, G. B. *J. Elastom. Plast.* **2012**, *44*, 189.
19. Kamaruddin, S.; Khan Z. A.; Foong, S. H. *IACSIT Int. J. Eng. Technol.* **2010**, *2*, 574.
20. Rafizadeh, M.; Morshedian, J.; Ghasemi, I.; Bolouri, A.; *Iran. Polym. J.* **2005**, *14*, 881.
21. Sureshkumar, M. S.; Naskar, K.; Nando, G. B.; Bhardwaj, Y. K.; Sabharwal, S. *Polym.-Plast. Technol. Eng.* **2008**, *47*, 341.
22. Jazani, O. M.; Arefazar, A.; Saeb, M. R.; Ghaemi, A. *J. Appl. Polym. Sci.* **2010**, *116*, 2312.
23. Shokoohi, S.; Arefazar, A.; Naderi, G.; *Mater. Des.* **2011**, *32*, 1697.
24. Khosrokhavar, R.; Naderi, G.; Bakhshandeh, G. R.; Ghoreishy, M. H. R. *Iran. Polym. J.* **2011**, *20*, 41.
25. Taguchi, G. In Introduction to Quality Engineering: Designing Quality into Products and Processes; Asian Productivity Organization: Tokyo, **1986**.
26. Fisher, R. A. In The Design of Experiments; Oliver & Boyd: Edinburgh, **1935**.
27. Taguchi, G. In Introduction to Quality Engineering: Designing Quality into Products and Processes; Asian Productivity Organization, Tokyo, Japan, **1986**.
28. Ross, P. J. In Taguchi Techniques for Quality Engineering: Loss Function, Orthogonal Experiments, Parameter and Tolerance Design; McGraw-Hill: New York, **1988**.
29. Taguchi, G.; Chowdhury, S.; Wu Y. In Taguchi's Quality Engineering Handbook; Wiley: New York, **2005**.
30. Phadke, M. S. In Quality Engineering Using Robust Design; Prentice Hall: New Jersey, **1989**.
31. Wysk, R. A.; Niebel, B. W.; Cohen, P. H.; Simpson T. W. In Manufacturing Process: Integrated Product and Process Design; McGraw-Hill: New York, **2000**.
32. Roy, R. K. In Design of Experiments Using the Taguchi Approach: 16 Steps to Product and Process Improvement; Wiley: New York, **2001**.
33. Stamatis, D. H. In Six Sigma and Beyond Design of Experiments; CRC Press: Florida, **2002**; Vol. *V*, Chapter 17, p 381.
34. Peterson, S.; Jayaraman, K.; Bhattacharyya D. *Compos. A* **2002**, *33*, 1123.
35. Reddy, M. M.; Mohanty, A. K.; Misra, M. *J. Mater. Sci.* **2012**, *47*, 2591.
36. Krishnaiah, K.; Shahabudeen, P. In Applied Design of Experiments and Taguchi Methods; PHI Learning: New Delhi, **2012**.
37. Dai, X.; Xu, J.; Guo, X.; Lu, Y.; Shen, D.; Zhao, N. Luo, X.; Zhang, X. *Macromolecules* **2004**, *37*, 5615.
38. Pattanayak, A.; Jana, S. C. *Polymer* **2005**, *46*, 3275.
39. Tien, Y. I.; Wei K. H. *Polymer* **2001**, *42*, 3213.
40. Pospíšil, M.; Čapková, P.; Měřínská, D.; Maláč, Z.; Šimoník, J. *J. Colloid Interface Sci.* **2001**, *236*, 127.
41. Paul, D. R.; Robeson, L. M. *Polymer* **2008**, *49*, 3187.
42. Barick, A. K.; Tripathy, D. K. *J. Appl. Polym. Sci.* **2010**, *117*, 639.
43. Barick, A. K.; Tripathy, D. K. *Appl. Clay Sci.* **2011**, *52*, 312.
44. Lee, K.-S.; Chang, Y.-W. *J. Appl. Polym. Sci.* **2012**. DOI: 10.1002/APP.38457.
45. Choi, M.-C.; Jung, J.-Y.; Yeom, H.-S.; Chang, Y.-W. *Polym. Eng. Sci.* **2012**. DOI: 10.1002/pen.23348.